

## Fracture of polypropylene: 2. The effect of crystallinity

A. van der Wal, J. J. Mulder and R. J. Gaymans\*

Twente University, Department of Chemical Technology, P.O. Box 217, Enschede, NL-7500 AE, The Netherlands

(Received 26 February 1997; revised 8 September 1997; accepted 5 November 1997)

The effect of crystallinity on the fracture behaviour of polypropylene was studied under impact conditions. The crystallinity was varied by taking low- and high-isotactic polypropylenes and mixtures thereof. The crystallinity ranged from 31 to 53 wt%. The fracture behaviour was studied as a function of temperature by means of a tensile test on notched Izod bars at  $1 \text{ m s}^{-1}$ . The brittle-to-ductile transition temperature ( $T_{bd}$ ) increases with increasing crystallinity, which is primarily attributed to the increasing yield stress. In the case of brittle fracture, the fracture energy decreases with increasing crystallinity. In the case of ductile fracture, the fracture energy seems to remain constant, irrespective of the crystallinity. © 1998 Elsevier Science Ltd. All rights reserved.

(Keywords: polypropylene; fracture; crystallinity)

### INTRODUCTION

The fracture behaviour of polypropylene depends on the test conditions and material properties, such as molecular weight and crystallinity. However, little attention has been paid to the effect of crystallinity.

The fracture behaviour of polypropylene was studied in detail as a function of molecular weight and temperature<sup>1</sup>. Under notched impact conditions, polypropylene undergoes a clear brittle-to-ductile transition at high temperatures (about 100°C), far above its glass transition temperature ( $T_g$ )<sup>1</sup>. The brittle-to-ductile transition temperature ( $T_{bd}$ ) decreases with increasing molecular weight, which is attributed to an increase in the fracture stress<sup>1</sup>.

The intrinsic crystallinity of polypropylene depends largely on the isotacticity. With increasing isotacticity, crystallinity increases<sup>2,3</sup>. The isotacticity is a measure of the stereoregularity of the polypropylene chain. In atactic polypropylene, the methyl group is randomly positioned on the chain backbone, whereas isotactic polypropylene possesses a methyl group at a regular position. Standard commercial polypropylene consists mainly of isotactic polypropylene. The effect of isotacticity on the crystallization behaviour has been studied extensively<sup>3–9</sup>. Keith and Padden<sup>4</sup> found a spherulitic structure over a wide range of isotacticity values. With increasing isotacticity the spherulites become more densely packed<sup>4</sup>. The spherulite size is not or is only slightly affected by isotacticity<sup>10,11</sup>.

A spherulite consists of fibrils which radiate from the centre. These fibrils are made up of stacks of lamellae. The amorphous phase is found in between the fibrils and in between the lamellae. Lohse *et al.*<sup>11</sup> studied the mixing of purely atactic and purely isotactic polypropylene. These stereoisomers mix in the melt, but are separated by crystallization. Atactic polypropylene is mainly found between the fibrils, but not between the lamellae.

In the present paper, the effect of crystallinity on the fracture behaviour of polypropylene is studied under impact

conditions. The crystallinity was varied by mixing low- and high-isotactic polypropylenes. Special attention is paid to the brittle-to-ductile transition.

### EXPERIMENTAL

#### Materials

The materials used in this study were a low-isotactic (Novolen 1300 L, BASF) and a high-isotactic polypropylene homopolymer (Eltex P HCS 580, Solvay). Both materials were kindly supplied by their producers and were used as delivered. *Table 1* lists the respective material properties. It should be noted that the materials have the same melt-flow index (MFI), which may indicate that their molecular weights are comparable. The modulus and the yield stress of standard polypropylene with the same MFI are 1500 and 34 MPa, respectively. These values are between those of the low- and high-isotactic polypropylenes.

#### Specimen preparation

The low- and high-isotactic polypropylenes were mixed on a co-rotating twin-screw extruder (Berstorff ZE 25, diameter = 25 mm, ratio of length/diameter = 33) to afford a series of polypropylenes with varying isotacticity. The barrel temperature and the screw speed were 200°C and 100 rev min<sup>-1</sup>, respectively. Rectangular bars (74 mm × 10 mm × 4 mm, ISO 180/1A) and dumbbell-shaped specimens (10 mm × 3 mm × 115 mm, ISO R527-1) were injection-moulded on an 221-55-250 Arburg Allrounder. The barrel temperature and screw speed were 230°C and 200 rev min<sup>-1</sup>, respectively. The mould temperature was 40°C. A single-edge 45° V-shaped notch (tip radius 0.25 mm, depth 2 mm) was milled in the bars. The material code in this context is EXX. E is the code for Eltex, while XX indicates the Eltex content (wt%).

#### Differential scanning calorimetry (d.s.c.)

Differential scanning calorimetry was carried out on a Perkin–Elmer DSC 7 instrument. Samples (about 10 mg)

\* To whom correspondence should be addressed

were taken from the core of the injection-moulded bars. The instrument was cooled with liquid nitrogen. Scans were recorded at a heating and cooling rate of  $20^{\circ}\text{C min}^{-1}$  over a temperature range between 60 and  $220^{\circ}\text{C}$ . Before heating and cooling, the starting temperature was maintained for 2 min. The melting and crystallisation temperature were defined as the peak temperature. Enthalpies were calculated from the peak area. As a baseline for determination of the melting peak area, the heat flow temperature line for the melt was extrapolated to lower temperatures.

#### Dynamical mechanical analysis (d.m.a.)

Dynamical mechanical analysis was performed on the gauge section of the dumbbell-shaped specimen ( $50\text{ mm} \times 10\text{ mm} \times 3\text{ mm}$ ) using a Myrenne ATM3 torsion pendulum. Single measurements were performed at 1 Hz at a heating rate of  $1.8^{\circ}\text{C min}^{-1}$ .

#### Tensile test

The tensile tests were carried out on dumbbell-shaped specimens on an Instron tensile machine. This test is described in detail elsewhere<sup>1</sup>. All measurements were performed six times.

#### Single-edge notched (SEN) tensile test

The fracture behaviour was studied by a tensile test on SEN bars<sup>1</sup>. The test was carried out five times.

The following parameters are used to describe the fracture process:

*maximum stress*: force maximum on the force–displacement curve, divided by the cross-sectional area behind the notch ( $32\text{ mm}^2$ );

*crack initiation displacement (CID)*: the clamp displacement to the moment of maximum force;

*crack initiation energy (CIE)*: the energy supplied to the moment of maximum force;

*crack propagation displacement (CPD)*: the difference in clamp displacement between the point of maximum force and the point of zero force;

*crack propagation energy (CPE)*: the difference in energy supplied between the point of maximum force and the point of zero force;

*fracture displacement*: the total displacement; and

*fracture energy*: the total energy.

## RESULTS AND DISCUSSION

### Materials

Low- and high-isotacticity polypropylenes were mixed to afford a series of polypropylenes with varying isotacticity. In the mixtures the isotacticity per individual chain probably shows a large distribution. As discussed in Section Section

**Table 1** Starting materials

Property	Units	Novolen 1300 L	Eltex P HCS 580
MFI ( $230^{\circ}\text{C}$ , 21.6 N)	$\text{dg min}^{-1}$	5	5
Density	$\text{kg m}^{-3}$	898	915
Yield stress <sup>a</sup>	MPa	21	40
Yield strain <sup>a</sup>	%	16	—
Tensile modulus <sup>b</sup>	MPa	650	2075

All data from data sheets<sup>12,13</sup>

<sup>a</sup>ISO R 527,  $50\text{ mm min}^{-1}$

<sup>b</sup>ISO R 527,  $1\text{ mm min}^{-1}$

1, chains with low isotacticity are mainly located in the amorphous phase in between the fibrils.

*D.s.c. and d.m.a.* The d.s.c. results for the different materials are listed in Table 2. The melting and crystallization enthalpy increases almost linearly with the Eltex content. The melting enthalpy of E67 corresponds to that of standard polypropylene<sup>1</sup>. The melting temperature increases slightly with the Eltex content, by contrast to the crystallization temperature, which increases considerably. The increase in the peak crystallization temperature was accompanied by an increase in the onset crystallization temperature.

The enthalpy of fusion for 100% crystalline polypropylene is almost independent of the isotacticity and equals  $207\text{ J g}^{-1}$  (<sup>3</sup>). The crystallinity of the specimens, based on  $\Delta H_{m,1}$ , as a function of the Eltex content is listed in Table 2. The crystallinity increases almost linearly with Eltex content, i.e. from 31 to 53 wt%.

D.m.a. (at 1 Hz) demonstrates that all tested materials have the same  $T_g$  of  $3 \pm 2^{\circ}\text{C}$ .  $T_g$  is defined as the peak temperature of the loss modulus.

### Storage modulus and tensile properties

*Storage modulus.* Figure 1 shows the storage modulus measured by d.m.a. at 1 Hz as a function of temperature. At temperatures below the glass transition temperature, the storage modulus is almost independent of the crystallinity. Above the glass transition temperature, the storage modulus increases with increasing crystallinity. D.m.a. measurements obtained by Flocke<sup>14</sup> showed the same tendency. The fact that, below  $T_g$ , the storage modulus is hardly affected by crystallinity suggests that the modulus of the amorphous phase below  $T_g$  is almost identical to the modulus of the crystalline phase.

*Tensile properties.* The tensile modulus, yield stress and yield strain as a function of crystallinity are shown in Table 3, which demonstrates that the yield stress of the

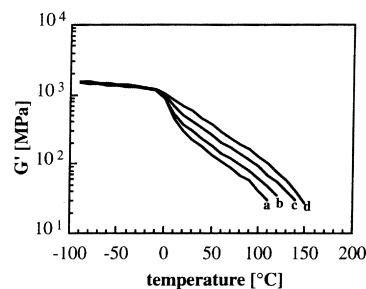


**Figure 1** The storage modulus ( $G'$ , 1 Hz) as a function of temperature for the polypropylenes.  $X_c$  (wt%): (a) 31, (b) 38, (c) 43, (d) 53

**Table 2** D.s.c. results for polypropylenes with varying isotacticity

Code	First heating			Second heating		Cooling	
	$T_{m,1}$ ( $^{\circ}\text{C}$ )	$\Delta H_{m,1}$ ( $\text{J g}^{-1}$ )	$X_c$ (wt%)	$T_{m,2}$ ( $^{\circ}\text{C}$ )	$\Delta H_{m,2}$ ( $\text{J g}^{-1}$ )	$T_c$ ( $^{\circ}\text{C}$ )	$\Delta H_c$ ( $\text{J g}^{-1}$ )
E0	166	64	31	166	66	100	74
E33	170	78	38	166	79	102	85
E67	169	88	43	168	93	111	96
E100	171	110	53	172	112	122	110

$X_c$ : degree of crystallinity ( $\Delta H_m^{\circ} = 207\text{ J g}^{-1}$  for 100% crystalline polypropylene)

starting materials almost equals the values quoted by the suppliers (Table 1). However, the tensile modulus is significantly lower than the given value, despite the higher test speed. The modulus and the yield stress increase almost linearly with increasing crystallinity. The modulus increases by a factor of 3 and the yield stress by a factor of 2. The decrease in yield strain with increasing crystallinity (by a factor of 4, Table 3) is much higher than the decrease in yield stress/modulus ratio (by a factor of 1.5). The yield strain of the lowest crystalline material (17%) corresponds to the supplier's value (Table 1).

#### SEN tensile test

The fracture behaviour was studied by an SEN tensile test at  $1 \text{ m s}^{-1}$ . The applied strain rate in this test is of the same order of magnitude as in an impact test<sup>1</sup>. The stress–displacement curves of E0 and E100 obtained by SEN tensile tests at different temperatures are shown in Figures 2 and 3. The fracture process may be divided into crack initiation and crack propagation stages. During crack initiation stress builds up at the notch tip, but is too low to enable crack propagation. Crack propagation is assumed to start at or just past the maximum stress<sup>1</sup>. In the brittle samples the materials fracture at or just past the maximum stress. The maximum stress for the ductile fracturing samples (at somewhat higher temperatures) is not higher than that for the brittle samples.

The samples tested at high test speeds often show a discontinuity in the stress–strain curve before the maximum stress is reached<sup>1</sup>. The origin of this discontinuity is thought to be a dynamic effect of the SEN test at these high test speeds.

At low temperatures crack propagation begins at the maximum stress (Figures 2 and 3). At higher temperatures,

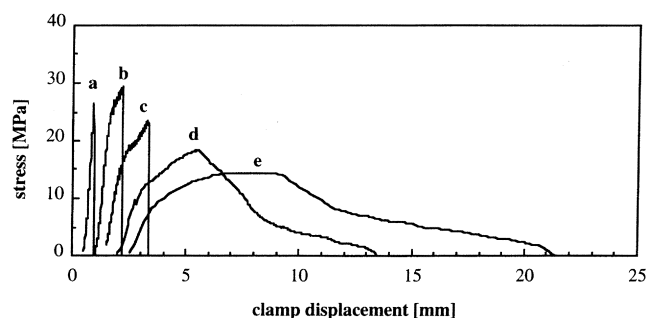


**Figure 2** Stress–displacement curves obtained by an SEN tensile test ( $1 \text{ m s}^{-1}$ ) for E0 ( $X_c = 31 \text{ wt}\%$ ). Temperature ( $^{\circ}\text{C}$ ): (a) 0, (b) 20, (c) 40, (d) 60, (e) 80

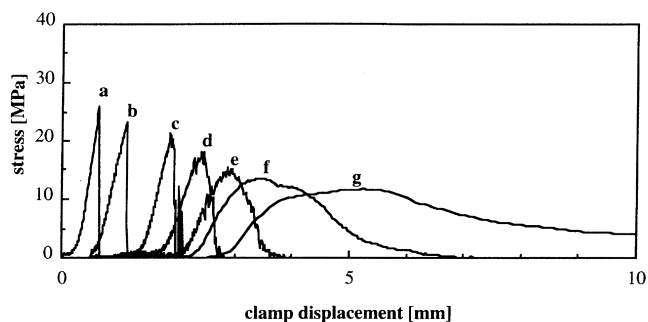


**Figure 3** Stress–displacement curves obtained by an SEN tensile test ( $1 \text{ m s}^{-1}$ ) for E100 ( $X_c = 53 \text{ wt}\%$ ). Temperature ( $^{\circ}\text{C}$ ): (a) 20, (b) 40, (c) 60, (d) 80, (e) 100, (f) 120, (g) 135

crack propagation begins beyond the maximum stress (Figures 2 and 3), and is preceded by yielding during crack initiation (Figures 2 and 3). The sharp drop in stress beyond the stress maximum at low temperatures indicates that no additional energy is needed for crack propagation. This type of fracture is referred to as brittle fracture. At high temperatures additional energy is needed for crack propagation. This type of fracture is referred to as ductile fracture.

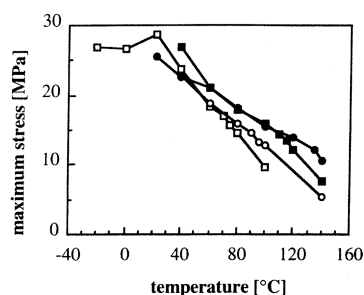
**Maximum stress.** ‘Maximum stress’ is defined as the maximum stress in the stress–displacement curve obtained by an SEN tensile test. Figure 4 shows the maximum stress as a function of temperature. This stress is the cross-sectional stress, neglecting stress concentration at the notch tip. Above  $20^{\circ}\text{C}$ , the maximum stress decreases with increasing temperature. At high temperatures, a change in slope in the maximum stress–temperature curve is observed for all materials (Figure 4). With increasing crystallinity this change in slope occurs at 70, 90, 110 and  $135^{\circ}\text{C}$ , respectively. As the slope changes, the failure mode changes from brittle to ductile<sup>1</sup>. Above  $60^{\circ}\text{C}$ , the fracture stress of the two materials with the highest crystallinity is slightly higher than that for the materials with the lowest crystallinity (Figure 4). Beyond the change in slope, the failure mode is ductile, and hence the maximum stress with increasing crystallinity (Figure 4).

Figure 5 shows crack initiation, crack propagation and fracture displacement. Figure 6 shows crack initiation, crack propagation and fracture energy. Crack propagation was assumed to start at the transition in the stress–displacement curve near the stress maximum. However, in the case of highly ductile fracture, no clear transition was observed and determination of the beginning of crack propagation was somewhat arbitrary.

**Crack initiation.** The crack initiation displacement and crack initiation energy increase with the temperature, passing through a maximum at high temperature, except for E100. Both CID and CIE decrease with increasing crystallinity.

**Crack propagation.** With increasing temperature the crack propagation displacement and crack propagation energy increase sharply from their previous zero level. With increasing crystallinity, the CPD–temperature curve shifts towards higher temperatures. For E33 and E67, with increasing temperature, the CPE passes through a maximum which was not observed for the CPD.

**Total fracture process.** Fracture displacement decreases with increasing crystallinity. In the case of brittle fracture



**Figure 4** Maximum stress during SEN tensile tests at  $1 \text{ m s}^{-1}$  versus temperature for the polypropylenes.  $X_c$  (wt%):  $\square$ , 31;  $\circ$ , 38;  $\blacksquare$ , 43;  $\bullet$ , 53. The stress is the cross-sectional stress, neglecting stress concentration at the notch tip

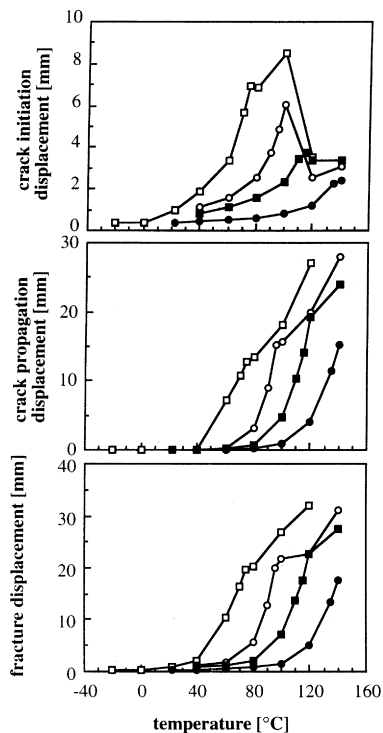


**Figure 5** Displacement during SEN tensile tests (at  $1 \text{ m s}^{-1}$ ) as a function of temperature for the polypropylenes.  $X_c$  (wt%):  $\square$ , 31;  $\circ$ , 38;  $\blacksquare$ , 43;  $\bullet$ , 53

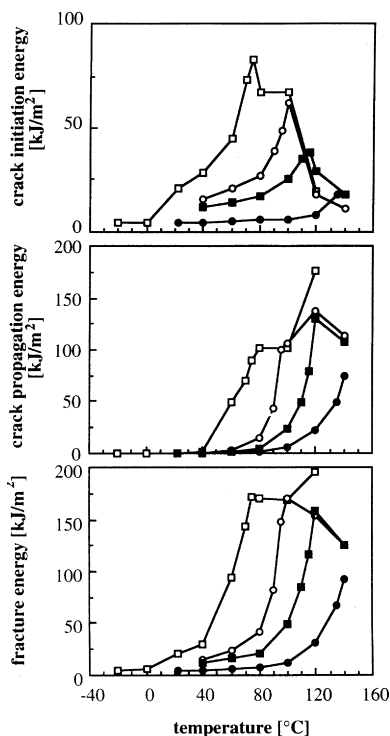


**Figure 6** Supplied energy during SEN tensile tests (at  $1 \text{ m s}^{-1}$ ) as a function of temperature for the polypropylenes.  $X_c$  (wt%):  $\square$ , 31;  $\circ$ , 38;  $\blacksquare$ , 43;  $\bullet$ , 53

the fracture energy decreases with increasing crystallinity, although, at ductile fracture, the fracture energy seems to remain constant irrespective of the crystallinity. As a first approximation, the fracture energy is assumed to be proportional to the product of fracture displacement and maximum stress. In the case of brittle fracture, the fracture energy decreases with increasing crystallinity, owing to a decrease

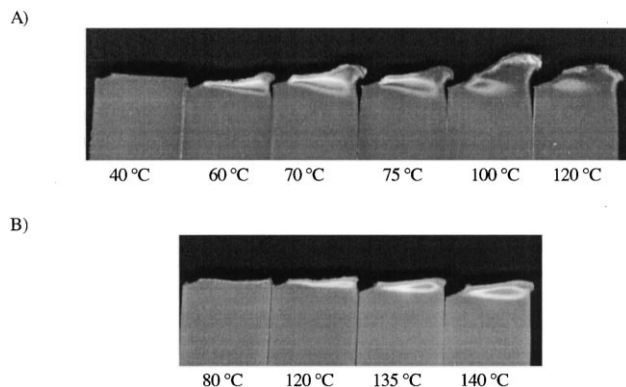


**Figure 7** Fractured specimens at different temperatures: (A) E0 ( $X_c = 31 \text{ wt\%}$ ); (B) E100 ( $X_c = 53 \text{ wt\%}$ )

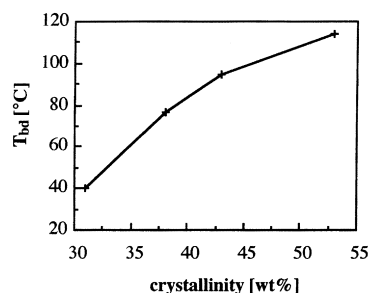


**Figure 8** The brittle-to-ductile transition temperature ( $T_{bd}$ ) as a function of crystallinity for polypropylene

**Table 3** Tensile properties of polypropylene (at  $50 \text{ mm min}^{-1}$ ) as a function of crystallinity

$X_c$ (wt%)	Modulus (MPa)	Yield stress (MPa)	Yield strain (%)
31	601	19.5	17.0
38	962	25.4	11.0
43	1228	31.9	8.8
53	1650	41.0	4.0

in fracture displacement. In the case of ductile fracture, the decrease in fracture displacement is apparently compensated by increasing maximum stress.

**Fracture surface.** E0 and E100 specimens fractured at various temperatures are shown in *Figure 7*. At low temperatures the specimens exhibit a flat fracture surface (*Figure 7A*,  $0^\circ\text{C}$  and *Figure 7B*,  $40^\circ\text{C}$ ). At higher temperatures, shear lips are formed for E0 at  $40^\circ\text{C}$  and for E100 at  $80^\circ\text{C}$  (*Figure 7A* *Figure 7B*). The size of the shear lips increases with increasing temperature (*Figure 7*). The plastic deformation at the fracture zone is accompanied by stress whitening, which disappears with increasing temperature and increasing plastic strain (*Figure 7B*,  $140^\circ\text{C}$ ).

The onset of shear-lip formation for E0 and E100 at  $40^\circ\text{C}$  and  $80^\circ\text{C}$  respectively is accompanied with the onset of the crack propagation energy (*Figure 6*). This indicates that energy absorption during crack propagation and ductile deformation, respectively, is due to pronounced plastic deformation during crack propagation. The same ductile deformation behaviour was found for E33 and E67.

**Brittle-to-ductile transition.** In this context, the brittle-to-ductile transition is defined as the onset of ductile fracture. The crack propagation energy is a measure of the

ductility of fracture. However, crack propagation displacement seems to be a more accurate measure<sup>P</sup>. The brittle-to-ductile transition temperature ( $T_{bd}$ ) is determined by extrapolating the linear part (between approximately 5 and 15 mm) in the CPD-temperature curve to zero. *Figure 8* shows the  $T_{bd}$  as a function of crystallinity.  $T_{bd}$  increases with increasing crystallinity.

Ductile deformation is due to pronounced plastic deformation during crack propagation. Plastic deformation occurs when the yield stress drops below the fracture stress. With increasing temperature, the yield stress decreases in relation to the fracture stress, leading to a brittle-to-ductile transition. With increasing crystallinity, the fracture stress increases slightly (*Figure 4*), and the yield stress increases strongly (*Table 3*). The overall effect of crystallinity is an increase in yield stress in relation to the fracture stress, resulting in an increase in  $T_{bd}$  with increasing crystallinity.

## CONCLUSIONS

The brittle-to-ductile transition temperature increases with increasing crystallinity, which is primarily attributed to the increasing yield stress. In the case of brittle fracture, the fracture energy decreases with increasing crystallinity. In the case of ductile fracture, the fracture energy seems to remain constant irrespective of the crystallinity.

## ACKNOWLEDGEMENTS

We would like to thank Prof. Dr. Ir. L. C. E. Struik for helpful discussions and comments. This work is part of the research programme of Twente University.

## REFERENCES

1. Van der Wal, A., Mulder, J. J., Thijs, H. A. and Gaymans, R. J., *Polymer*, 1998, **39**, 5467.
2. Ibadon, A. O., *J. Appl. Polym. Sci.*, 1992, **46**, 2123.
3. Cheng, S. Z. D., Janimak, J. J., Zhang, A. and Hsieh, E. T., *Polymer*, 1991, **32**, 648.
4. Keith, H. D. and Padden, F. J. Jr., *J. Appl. Phys.*, 1964, **35**, 1270.
5. Keith, H. D. and Padden, F. J. Jr., *J. Appl. Phys.*, 1964, **35**, 1286.
6. Janimak, J. J., Cheng, S. Z. D. and Hsieh, E. T., *Macromolecules*, 1991, **24**, 2253.
7. Janimak, J. J., Cheng, S. Z. D., Zhang, A. and Hsieh, E. T., *Polymer*, 1992, **33**, 728.
8. Martuscelli, E., Pracella, M. and Crispino, L., *Polymer*, 1983, **24**, 693.
9. Martuscelli, E., Avella, M., Segre, A. L., Rossi, E., Di Drusco, G., Galli, P. and Simonazzi, T., *Polymer*, 1985, **26**, 259.
10. Friedrich, K., *Progr. Coll. Polym. Sci.*, 1979, **66**, 299.
11. Lohse, D. J. and Wissler, G. E., *J. Mater. Sci.*, 1991, **26**, 743.
12. *Novolen*. BASF Kunststoffe, Ludwigshafen, May 1991.
13. *Eltex P*. Solvay Polypropylene, May 1989.
14. Flocke, H. A., *Kolloid Z. Z. Polym.*, 1962, **180**, 118.